99

LA-UR- 01-0644

Approved for public release;
distribution is unlimited.

Title: RAPIDLY RE-COMPUTABLE EEG (ELECTROENCEPHALOGRAPHY) FORWARD MODELS FOR REALISTIC HEAD SHAPES

Author(s): John J. Ermer, University of Southern California
Richard M. Leahy, University of Southern California
John C. Mosher, NIS-9
Sylvain (nmi) Baillet, CNRS-Paris, France

Submitted to: 12th International Conference on Biomagnetism, Helsinki University of Technology, Espoo, Finland.

Los Alamos
NATIONAL LABORATORY

Rapidly Re-computable EEG Forward Models for Realistic Head Shapes

John J. Ermer[1], Richard M. Leahy[1], John C. Mosher[2], and Sylvain Baillet[1,3]

[1]*Signal & Image Processing Institute, University of Southern California, Los Angeles, CA USA*
[2]*Los Alamos National Laboratory, Los Alamos, NM 87545*
[3]*Hopital de la Salpetriere, CNRS-LENA, Paris, France*

1. Introduction

Solution of the EEG source localization (inverse) problem utilizing model-based methods typically requires a significant number of forward model evaluations. For subspace based inverse methods like MUSIC [6], the total number of forward model evaluations can often approach an order of 10^3 or 10^4. Techniques based on least-squares minimization may require significantly more evaluations.

The observed set of measurements over an M-sensor array is often expressed as a linear forward spatio-temporal model of the form:

$$F = GQ + N \qquad (1)$$

where the observed forward field **F** (M-sensors x N-time samples) can be expressed in terms of the forward model **G**, a set of dipole moment(s) **Q** (3xP-dipoles x N-time samples) and additive noise **N**.

Because of their simplicity, ease of computation, and relatively good accuracy, multi-layer spherical models [7] (or fast approximations described in [1], [7]) have traditionally been the "forward model of choice" for approximating the human head. However, approximation of the human head via a spherical model does have several key drawbacks.

By its very shape, the use of a spherical model distorts the true distribution of passive currents in the skull cavity. Spherical models also require that the sensor positions be projected onto the fitted sphere (Fig. 1), resulting in a distortion of the true sensor-dipole spatial geometry (and ultimately the computed surface potential). The use of a single "best-fitted" sphere has the added drawback of incomplete coverage of the inner skull region, often ignoring areas such as the frontal cortex. In practice, this problem is typically countered by fitting additional sphere(s) to those region(s) not covered by the primary sphere. The use of these additional spheres results in added complication to the forward model.

Using high-resolution spatial information obtained via X-ray CT or MR imaging, a realistic head model can be formed by tessellating the head into a set of contiguous regions (typically the scalp, outer skull, and inner skull surfaces). Since accurate *in vivo* determination of internal conductivities is currently not currently possible, the head is typically assumed to consist of a set of contiguous isotropic regions, each with constant conductivity.

With the exception of simple multilayer surfaces (spheres, ellipsoids), the analytical solution for the surface potential over an arbitrarily shaped multilayer surface is not known. For a surface of arbitrary shape, the surface potential can be found by solving Green's theorem (2) using the Boundary Element Method (BEM) or similar numerical techniques (*cf.* [5]).

$$\sigma_0 v_\infty(\boldsymbol{r}) = \frac{(\sigma_j^- + \sigma_j^+)}{2} v(\boldsymbol{r}) + \frac{1}{4\pi} \sum_{i=1}^{m} (\sigma_i^- - \sigma_i^+) \int_{S_i} \left(v(\boldsymbol{r}') \boldsymbol{n}_i(\boldsymbol{r}') \bullet \frac{(\boldsymbol{r} - \boldsymbol{r}')}{\|\boldsymbol{r} - \boldsymbol{r}'\|^3} \right) d\boldsymbol{r}' \quad , \boldsymbol{r} \in S_j \qquad (2)$$

The major drawback of BEM (and other numerical techniques) is their computational requirements, which can be in excess of 3 orders of magnitude over that of traditional multi-layer sphere models [3]. These extreme computational requirements usually prohibit the practical application of BEM in solving the EEG source localization problem. Lack of computationally efficient EEG forward modeling solutions (for non-spherical surfaces) appears to be the major barrier to widespread adaptation of realistic head models.

Past work in the area of computationally efficient EEG forward models has primarily focused on multilayer spherical models; most notably [1], [2], and [7]. For realistic head models, Huang et. al. [3] present a sensor-fitted sphere method for MEG whose accuracy approaches that of BEM with a computational cost on the order of a multilayer sphere. A survey of several BEM solutions and methods for minimizing runtime computations is presented in [5].

We present a straightforward method which allows for rapid evaluation of the EEG forward model over a realistic head shape. The quality of the

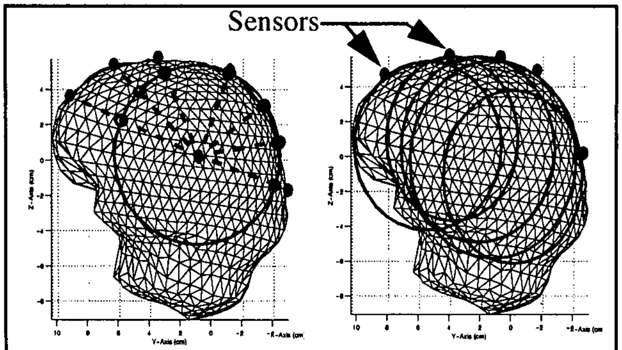

Figure 1: *(Left) Spatial distortion true sensor positions (●) due to radial projection onto best-fit single-sphere model (O). (Right) Schematic plot of sensor-weighted sphere model.*

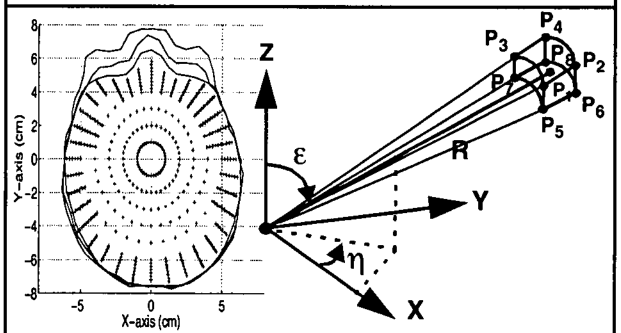

Figure 2: *(Left) Spherical grid points shown at level Z=0. (Right) Forward field interpolation based on weighted sum of 8 nearest grid points.*

forward modeling solution is shown to approach that of BEM, with re-computation time ~30x faster than that of a traditional multilayer spherical model. The proposed methodology has the added benefit of providing whole-head coverage.

2. Methods

In this study, we focused on two candidate methodologies: 1) Adaptation of the MEG sensor-fitted sphere methodology described by Huang et. al. [3] to EEG; 2) Calculation of the forward-field at an arbitrary dipole position via 3-D interpolation of the forward field over a pre-computed "grid."

2.1. Sensor-Fitted Sphere

A schematic diagram of the sensor-fitted sphere model described in [3] is shown in Fig. 1. The objective of this method is to determine the center and radii of the fitted-sphere which best approximates the true lead field for each individual sensor.

The lead field for each sensor is first computed using the Linear Galerkin BEM form [5] over a representative grid of dipoles. Assuming fixed conductivity values and proportional sphere radii, we find the center C_0 and outer radii R_0 of the multilayer sphere (for the m-th sensor) whose lead field which minimizes the function

(3)

The EEG sensor-fitted sphere model is then expressed as:

(4)

2.2. 3-D Forward Field Interpolation

The 3-D Forward-Field Interpolation method is illustrated in Fig. 2. In this method, a set of radially sampled (η,ε,R) grid points is established throughout the inner-skull cavity. In our study, both η and ε dimensions were sampled at 10^{o} intervals. The range dimension was sampled at fine intervals of 2mm when within 1-2cm of the inner surface boundary and at 1cm intervals elsewhere. Finer range resolution was utilized in the vicinity of the surface boundary to account for increased potential function sensitivity.

During the "pre-computation" phase, a high-resolution forward model is used to compute the (M x 3) forward field at each grid position. The final result is then stored as an indexed table.

For our high-fidelity forward model, we utilized BEM methods described in Mosher et. al. [5]. This included Constant Galerkin and Linear Galerkin forms of BEM.

At "run-time," the EEG forward model at an arbitrary location is determined via 3-D linear interpolation of the forward-field solution corresponding to the 8 nearest grid points (Fig. 2).

3. Results

The following metrics are used to evaluate pair-wise forward-field scale and subspace errors associated with two forward gain matrices and , where represents the best estimate of "truth." We define the (M-sensor x 1) forward field gain vector for the n-th elemental dipole as , where the n=1,...,3P elemental dipoles correspond to the x, y, and z Cartesian components for each of the P dipoles.

<u>Pairwise Forward Field PVU</u>: The purpose of this metric is to evaluate scale error and serve as a predic-

tor of forward model performance using least-squares based approaches where $0 \le PVU \le 1$.

$$PVU(n) = \frac{\left|g_B(n) - g_A(n)\right|^2_{Fro}}{\left|g_A(n)\right|^2_{Fro}} \qquad n = 1, \ldots, 3P \quad (5)$$

Pairwise Forward Field Subspace Correlation: The purpose of this metric is to evaluate subspace error and serve as a predictor of forward model performance using subpace-based approaches.

$$SBC_{FF}(n) = subcorr(g_A(n), g_B(n)) \quad n = 1, \ldots, 3P \quad (6)$$

where subcorr(**a**,**b**) represents the cosine of the principle angle between the vectors **a** and **b**.

3.1. Spherical Model Comparisons

In order to evaluate the impact of linear interpolation on EEG forward modeling error, we conducted a simple experiment using a 3-layer sphere of increasing radii 8.1, 8.5, 8.8 cm with conductivities 0.33, 0.0042, 0.33 mhos respectively. A 3-D interpolative grid was set up using the sampling density described in Section 2.2.

A set of dipoles falling at the center of each voxel (see Fig. 2) was then generated. Dipoles within 3mm of the inner layer boundary were included to simulate cortical responses. The true forward model for each dipole was computed using an analytical multilayer sphere model. Interpolated solution performance was then evaluated using the PVU and subcorr metrics described in section 3.0.

While not shown here, pairwise scale and subspace errors were found to be extremely small (PVU<0.01 and subcorr>0.99) for all elemental dipoles. The conclusion is that linear interpolation of the forward-field over a reasonably dense grid imposes little distortion in the original solution.

3.2. Phantom Model Comparisons

Surface data from the human skull phantom described in Leahy et. al. [4] was used to evaluate algorithm performance over a realistic head shape. Using X-ray CT data, three surfaces (inner-skull, outer-skull, scalp) were tessellated to a density of 1016 triangles per layer. A representative set of 1822 "test" dipole locations (5466 elemental dipoles) were generated, where all dipoles were internal to both the inner skull and "best-fitted sphere" volumes. In order to evaluate model performance in the cortical region, dipole positions were allowed to fall within 3mm of inner skull boundary. The sensor array consisted of 54 sensors distributed uniformly over the upper portion of the phantom scalp.

Table 1: *Computation and Memory Comparisons*

EEG Forward Model Method	One-Time Pre-Calculations (Sec)	Memory Storage (MB)	1622 Dipole Evaluation Time (Sec)
BEM (Constant Galerkin)	3,141.5	2.6	490.9
BEM (Linear Galerkin)	24,778.3	2.6	1,667.6
3-Layer Sphere N=100 Legendre	0.0	0.0	41.2
3-Layer Sphere Berg Approx.	34.2	0.0	2.36
Sensor Fitted Spheres	23,035.7	0.0	5.97
3-D Interpolation (Constant Galerkin BEM)	5,748.1	11.7	1.34
3-D Interpolation (Linear Galerkin BEM)	33,712.6	11.7	1.34

In order to establish a best estimate of EEG Forward model "truth," the Linear Galerkin BEM solution was computed for each test dipole. As cited in [5], the Linear Galerkin method was shown to provide solutions with an effective PVU error of <0.01.

Scale (PVU) and subspace (subcorr) error metrics for each elemental dipole are shown in Fig. 3 for various forward models.

3.3. Computational & Memory Comparisons

Timing and memory metrics for various EEG forward modeling methods are shown in Table 1. All benchmarks were determined running Matlab based programs on a 500 MHz Pentium P-III PC w/ 512MB RAM.

4. Discussion

With well-known surface extraction techniques readily available for MRI/X-ray CT modalities, the major obstacle in widespread application of realistic EEG head models is a lack of computationally efficient forward models.

Based on multilayer sphere and realistic phantom experiments, we observed that 3-D interpolation of the EEG forward-field over a reasonably sampled grid to be an exceptional approximation to the original forward-field function. This was found to be true even in cortical based regions within 3mm of the surface boundary. Exceptions were found only in extreme cases near rapidly changing surface boundaries (i.e. eye socket region) where the numerical solution becomes more non-linear.

Computationally, we found the spherical 3-D forward-field interpolation method to be in excess of 30x faster than that obtained using a traditional multilayer spherical forward model. We note that forward model re-computation time using the 3-D interpolation model is independent of the model chosen. Cast in this framework, high fidelity numerical solutions currently viewed as "computationally prohibitive" for solving the inverse problem (i.e. Linear Galerkin BEM [5]) can be rapidly re-computed in a highly efficient manner. In addition, one-time pre-calculations and table memory storage requirements were also found to be reasonable by today's computing standards.

Figure 3: *(Left) Pair-wise forward-field PVU (Left) and Pairwise forward-field subspace correlation (Right) between candidate forward model and Linear Galerkin BEM.*

Pairwise PVU (Forward-Field)	**Pairwise subcorr(v1,v2) (Forward-Field)**

3-Layer Sphere

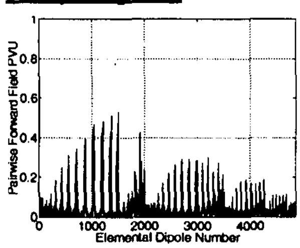

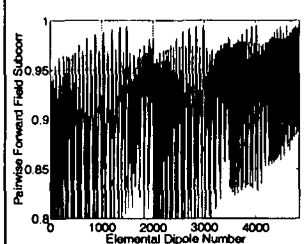

Sensor-Fitted Sphere

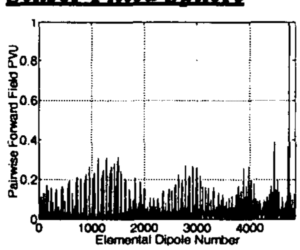

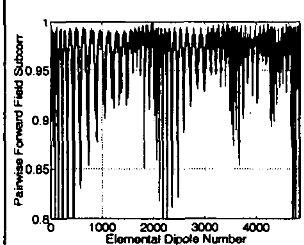

3-D Interpolation
(Constant Galerkin BEM)

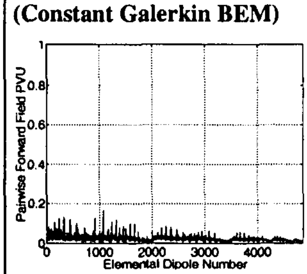

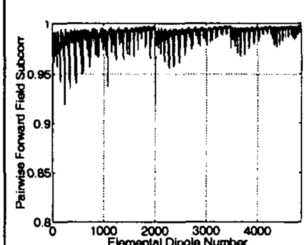

3-D Interpolation
(Linear Galerkin BEM)

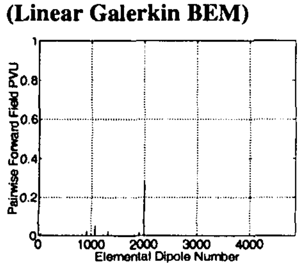

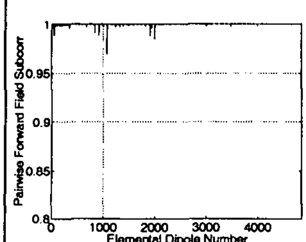

Performance wise, each of the 3-D Spherical Interpolation models shown in Fig. 3 were found to significantly outperform the multi-layer sphere model in terms of subspace error. Constant and Linear Galerkin BEM forms were observed to have subspace correlations better than 0.95 in nearly all cases. In comparison, the subspace correlations using a best-fitted multilayer sphere often fell below 0.9. A reduction in PVU scale error was also observed. A somewhat less dramatic EEG fwd modeling improvement was obtained using the fitted-sphere approach.

Furthermore, realistic EEG forward models have the added advantage of being defined over the whole head. In comparison, the surface potential for a dipole located external to a locally-fitted sphere, yet still internal to the skull, is undefined in a fitted sphere model.

Although the methods presented in this paper focus on the EEG forward model, they have also been applied to MEG with similar results.

5. References

[1] P. Berg and M. Scherg, "A fast method for forward computation of multiple-shell spherical head models", in Electroenceph. Clin. Neurophysiol, Vol. 90, 1994, pp. 58-64.

[2] J. deMunck, M. Peters, "A fast method to compute the potential in the multisphere model", IEEE Trans. Biomed. Eng. Vol 40, 1993, pp. 1166-1174.

[3] M.X. Huang, et. al., "A Sensor-Weighted Overlapping-Sphere Head Model and Exhaustive Head Model Comparison for MEG", Phys. Med. Biol Vol. 44, 1999, pp. 423-440.

[4] R.M. Leahy et. al., "A Study of Dipole Localization Accuray for MEG and EEG using a Human Skull Phantom", in Electroenceph. Clin. Neurophysiol, Vol. 107, 1998, pp. 159-173.

[5] J.C. Mosher, R.M. Leahy, and P.S. Lewis, "EEG and MEG: Forward Solutions for Inverse Methods", in IEEE Trans. Biomed. Eng. Vol 46, March 1999, pp. 245-259.

[6] J.C. Mosher, P.S. Lewis, and R.M. Leahy, "Multiple Dipole Modeling and Localization from Spatio-Temporal MEG Data", in IEEE Trans. Biomed. Eng. Vol 39, June 1992, pp. 541-557.

[7] Z. Zhang, "A Fast Method to Compute Surface Potentials Generated by Dipoles Within Multilayer Anisiotropic Spheres", Phys. Med. Biol Vol. 40, May 1995, pp. 335-349.